Shell-model description of high-spin states in ^{91}Nb

P. Dey[1],* R. Palit[1], P. C. Srivastava[2], Biswajit Das[1], S. V. Jadhav[1], A. Kundu[1], Md. S. R. Laskar[1], V. Malik[1], B. S. Naidu[1], D. Negi[1], and A. T. Vazhappilly[1]

[1]*Department of Nuclear and Atomic Physics, Tata Institute of Fundamental Research, Mumbai - 400005, INDIA and*
[2]*Department of Physics, Indian Institute of Technology Roorkee, Roorkee - 247667, INDIA*

Introduction

Nuclei near closed shell are of special interests in nuclear structure studies as they provide a platform for verification of shell-model (SM) calculations. Excited states in these nuclei help in understanding the effective interactions and extended model space used in modern SM calculations. High spin structures in $A \sim 90$ region have been observed to develop states having multiquasiparticle configurations with $g_{9/2}$ orbital playing a significant role. The effect of $\pi[1g_{9/2}]$ orbital comes into picture either due to the proton occupancy of the orbital or due to excitations of protons from the fp orbitals into the $g_{9/2}$ orbital across the $Z = 40$ subshell gap. These proton-excited configurations dominate the lower-energy part of the level scheme. However, it seems inadequate for describing high-spin states, where the role of $\nu[1g_{9/2}]$ orbital due to excitation across the $N = 50$ shell gap into the gd orbitals increases. Recently, the presence of $M1$ sequences at high-spin states in ^{90}Zr has been observed, originating from the recoupling of these proton and neutron configurations [1]. Being an $N = 50$ isotone, ^{91}Nb also provides a suitable testing ground to invoke the proton and neutron excitations simultaneously, which is the main motivation of the present study.

Experimental details and Results

Heavy-ion induced fusion-evaporation reactions ^{65}Cu(^{30}Si, $2p2n$)^{91}Nb have been performed to populate excited states in ^{91}Nb. 120 MeV ^{30}Si beam was provided by the TIFR-BARC PLF and 1 mg/cm^2 thick ^{65}Cu target with Au-backing was used. γ-rays emitted were detected by INGA consisting of 16 clover HPGe detectors placed at 5 different angles w.r.t the beam direction. Two- and higher-fold coincidence events sorted into various $E_\gamma - E_\gamma$ matrices and $E_\gamma - E_\gamma - E_\gamma$ cube, and, have been analyzed using the RADWARE packages [2].

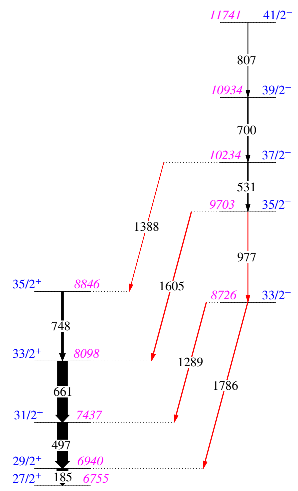

FIG. 1: Partial level scheme of ^{91}Nb. Newly observed transitions are marked in red color. The energies are rounded off to nearest integers.

The placement of transitions have been confirmed through their coincidence relationships and intensity measurements (shown in FIG. 1). The spin-parity of different states have been established on the basis of angular correlation and polarization measurements. 185-, 497-, 661- and 748-keV γ-transitions are identified as $M1$, therefore making them part of positive-parity sequence starting from 6755 keV, $27/2^+$ state. A new level at $E_x = 8726$ keV is identified as $33/2^-$ state through the $E1$ assignment of newly observed 1289-keV transition decaying to the $31/2^+$ state. Although, 531-, 700- and

*Electronic address: `piku.dey@tifr.res.in`

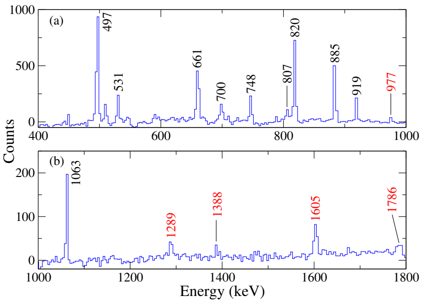

FIG. 2: Representative spectrum showing the sum of double-gated spectra with one gate on 422- (not shown in the level scheme) and other on 185-, 497- and 661-keV transitions. The newly observed transitions in ^{91}Nb are labeled in red.

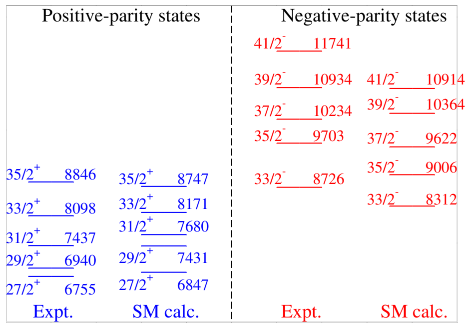

FIG. 3: Comparison of the experimental excitation energies and SM calculations both for positive and negative parity states.

807-keV were reported earlier [3], in our study, we have rearranged their placements in the proposed level scheme. These three transitions along with a newly observed 977-keV transitions form negative-parity sequence starting from 8726 keV state. Additionally, a few linking transitions between both sequences have been observed for the first time in this work.

Shell-model description

To understand the structure of these states, We have performed shell-model calculations using the GWBXG effective interaction with ^{68}Ni core. The GWBXG interaction has $\pi[1f_{5/2}, 2p_{3/2}, 2p_{1/2}, 1g_{9/2}]$ and $\nu[2p_{1/2}, 1g_{9/2}, 1g_{7/2}, 2d_{5/2}, 2d_{3/2}, 3s_{1/2}]$ orbitals. The single-particle energies (in MeV) used in this interaction are $\varepsilon^{\pi}_{1f_{5/2}} = -5.322$, $\varepsilon^{\pi}_{2p_{3/2}} = -6.144$, $\varepsilon^{\pi}_{2p_{1/2}} = -3.941$, $\varepsilon^{\pi}_{1g_{9/2}} = -1.250$ for the proton orbitals, and $\varepsilon^{\nu}_{2p_{1/2}} = -0.696$, $\varepsilon^{\nu}_{1g_{9/2}} = -2.597$, $\varepsilon^{\nu}_{1g_{7/2}} = +5.159$, $\varepsilon^{\nu}_{2d_{5/2}} = +1.830$, $\varepsilon^{\nu}_{2d_{3/2}} = +4.261$, $\varepsilon^{\nu}_{3s_{1/2}} = +1.741$ for the neutron orbitals. In our calculations for the neutrons we have completely filled $2p_{1/2}$, while we have not allowed any neutrons to occupy in $1g_{7/2}$ and $2d_{3/2}$ orbitals. Further, since the dimension is very large, we have allowed a maximum of one neutron each in the $2d_{5/2}$ and $3s_{1/2}$ orbitals. Calculations are performed with the shell-model code KSHELL [4].

The partial level scheme proposed here shows $M1$ sequences of both parities at high-spin. Positive- and negative-parity states in these sequences have $\pi[(1f_{5/2}2p_{1/2})^{-2}(1g_{9/2})^{3}] \otimes \nu[(1g_{9/2})^{-1}(2d_{5/2})^{1}]$ and $\pi[(1f_{5/2})^{-1}(2p_{1/2})^{-2}(1g_{9/2})^{4}] \otimes \nu[(1g_{9/2})^{-1}(2d_{5/2})^{1}]$ as the most dominant configurations, respectively. These configurations have stretched proton and neutron configurations, and high spin is generated by their recoupling. States of both parities up to highest observed excitation energies and spins indicate the dominance of single-particle excitations in this nucleus.

Acknowledgments

The authors are thankful to the staffs at TIFR-BARC PLF for providing a good-quality beam and smooth operation of the accelerator for the entire duration of the experiment. This work is supported by the Department of Atomic Energy, Government of India (Project Identification Code: 12-R&D-TFR-5.02-0200).

References

[1] P. Dey *et al.*, PRC **105**, 044307 (2022).
[2] D. C. Radford, NIM A **361**, 297 (1995).
[3] P. W. Luo *et al.*, PRC **89**, 034318 (2014).
[4] N. Shimizu *et al.*, Comput. Phys. Commun. **244**, 372 (2019).